

Empirical and mechanistic models for the particle export ratio

John P. Dunne,¹ Robert A. Armstrong,² Anand Gnanadesikan,^{1,2} and Jorge L. Sarmiento³

Received 20 October 2004; revised 16 September 2005; accepted 25 October 2005; published 30 December 2005.

[1] We present new empirical and mechanistic models for predicting the export of organic carbon out of the surface ocean by sinking particles. To calibrate these models, we have compiled a synthesis of field observations related to ecosystem size structure, primary production and particle export from around the globe. The empirical model captures 61% of the observed variance in the ratio of particle export to primary production (the *pe* ratio) using sea-surface temperature and chlorophyll concentrations (or primary productivity) as predictor variables. To describe the mechanisms responsible for *pe*-ratio variability, we present size-based formulations of phytoplankton grazing and sinking particle export, combining them into an alternative, mechanistic model. The formulation of grazing dynamics, using simple power laws as closure terms for small and large phytoplankton, reproduces 74% of the observed variability in phytoplankton community composition wherein large phytoplankton augment small ones as production increases. The formulation for sinking particle export partitions a temperature-dependent fraction of small and large phytoplankton grazing into sinking detritus. The mechanistic model also captures 61% of the observed variance in *pe* ratio, with large phytoplankton in high biomass and relatively cold regions leading to more efficient export. In this model, variability in primary productivity results in a biomass-modulated switch between small and large phytoplankton pathways.

Citation: Dunne, J. P., R. A. Armstrong, A. Gnanadesikan, and J. L. Sarmiento (2005), Empirical and mechanistic models for the particle export ratio, *Global Biogeochem. Cycles*, 19, GB4026, doi:10.1029/2004GB002390.

1. Introduction

[2] Understanding the sensitivity and adaptability of ecosystems to environmental change requires the development of models of oceanic ecosystems that are simple enough to be embedded in large-scale general circulation models, yet are robust and representative enough to be applied over the entire globe. In order for these models to be viable, they must be able to reproduce large-scale biogeochemical processes in robust ways with a minimum of complexity. A particularly important quantity in this respect is the ratio between the export of rapidly sinking particulate matter (particle export) and the total production of organic matter by photosynthesis (primary production), the *pe* ratio. While there is a considerable literature on the estimation of primary production, both in situ and from space (through chlorophyll-based algorithms), far less is understood about the connection between primary production and particle export, though a diversity of approaches

to link primary production to the cycling of carbon have been pursued.

[3] In one such approach [Dugdale and Goering, 1967], the portion of primary production driven by externally supplied nutrients (“new” production) is distinguished from that fueled by “regenerated” nutrients; the resulting ratio of “new” production to total primary production is defined as the “*f* ratio.” Assuming a steady state nutrient budget for the euphotic zone with constant elemental stoichiometry of organic material and an absence of nitrate regeneration in the euphotic zone, “new” production can be equated with export production. Eppley and Peterson [1979] synthesized a large number of measurements of the *f* ratio and found a strong dependence on primary production. They proposed a generalization in which waters with low levels of primary production have low *f* ratios, while waters with high levels of production have much higher *f* ratios, saturating at 0.5.

[4] Subsequent studies attempted to improve on this parameterization by approaching the problem from the export side using sediment trap data. Suess [1980] demonstrated that the sinking particle flux could be estimated as a function of primary production and depth. Subsequent studies such as those of Betzer *et al.* [1984], Pace *et al.* [1987] and Wassman [1990] further investigated this relationship. Bishop [1989] used a broad synthesis to compare these approaches, demonstrating that while particle flux attenuation with depth beneath the euphotic zone was fairly well constrained by the sinking particle flux out of the

¹NOAA Geophysical Fluid Dynamics Laboratory, Princeton, New Jersey, USA.

²Marine Sciences Research Center, Stony Brook University, Stony Brook, New York, USA.

³Atmospheric and Oceanic Sciences Program, Princeton University, Princeton, New Jersey, USA.

euphotic zone, the link to primary production was much more uncertain.

[5] Improvement of the f ratio based approaches also continued, taking particular advantage of the advent of trace-metal clean techniques for measuring primary production. *Platt and Harrison* [1985] developed an exponential saturation of the f ratio as a function of nitrate concentration (i.e., $1 - e^{-k \text{NO}_3^-}$) that applied to conditions of very low ammonium concentration ($<0.1 \mu\text{M NH}_4^+$). *Harrison et al.* [1987] expanded this nutrient-based approach; by assuming that the uptake rate constants of nitrate and ammonium were equivalent, they arrived at a form for the f ratio of $\text{NO}_3^-/(\text{NH}_4^+\text{NO}_3^-)$. The role of ammonium was further explored and confirmed in the multiple linear regression work of *Aufdenkampe et al.* [2001]. *Baines et al.* [1994] developed an algorithm to predict particle export directly from phytoplankton biomass alone. *Tremblay et al.* [1997] found a linear relationship between the f ratio and the fraction of large phytoplankton through an analysis of size-fractionated ($>5 \mu\text{m}$) biomass and primary production measurements.

[6] Ecosystem modeling studies have attempted to simulate variability in the f ratio and pe ratio mechanistically in terms of phytoplankton-zooplankton interactions [*Aksnes and Wassmann*, 1993] and within phytoplankton models that include size-dependence [e.g., *Legendre and Rassoulzadegan*, 1996; *Legendre*, 1998]. One class of such models (exemplified by the classic work of *Fasham et al.* [1990]) involves phytoplankton, zooplankton, detritus, bacteria, dissolved organic matter and two inorganic (nitrate and ammonium) species. *Laws et al.* [2000] were able to take a major step forward in elucidating the link between primary production and particle export. Rather than using a fully dynamical ecosystem model to predict export, they chose the more limited objective of constructing a steady state transfer function between primary productivity and export production. Their model predicts an abrupt switching between high and low pe -ratio pathways of conversion to sinking particles; under such conditions, high f ratios are never achieved at high temperatures.

[7] In this communication, we build upon previous efforts to determine the relationship between primary production and the sinking flux of particles. We first synthesize field observations related to ecosystem size structure, primary production and particle export from around the globe. Second, we perform an empirical, statistical assessment of this global data compilation to develop an empirical algorithm for the pe ratio for global application. This exercise uses a wide range of predictor variables in multiple combinations, both to assess what are the most important variables and to assess the level of prediction (explained variance) that could be expected from a model. Third, we utilize the same global data compilation to calibrate a mechanistic model of ecosystem dynamics based on grazing control of phytoplankton community size structure. We do this by distinguishing “small” phytoplankton (e.g., *Prochlorococcus*, *Synechococcus*, and a portion of the picoeukaryotes community) that constitute a fraction that forms the base of the microbial loop from “large” phytoplankton species (e.g., diatoms) that are much more predisposed to sinking through a variety of mechanisms. In this model, zooplankton grazing

pressure is treated implicitly to keep pace with small phytoplankton production while not keeping pace with large phytoplankton production. We then describe a means of modeling the pe ratio as a function of the relative abundances and productivities of “small” and “large” phytoplankton and demonstrate the broad robustness of the resulting algorithm. Finally, we discuss the implications for this work for our understanding of the underlying controls on particle export and the limitations of this approach.

2. Data Synthesis

[8] We compiled available field observations of primary production and particle export from approximately 40 oceanographic studies, which we have divided into 122 independent observations of ecosystem state. In order to maximize global coverage, we include data from estimates of “new” (NO_3^- -based) production, nutrient, oxygen or carbon based estimates of export production, and particle export estimates based on sinking flux from sediment traps and/or ^{234}Th . In cases where sampling was performed intensively at a single location rather than at geographically and temporally random sites, we grouped ecologically similar conditions in order to preserve the natural variability in the observations without excessively weighting individual locations. In order to combine data taken using different methods, it was necessary to either explicitly account for temporal variability or to assume a “steady state,” defined for our purposes as a condition wherein the change in phytoplankton biomass over time is small relative to primary production. In studies in which nonsteady state conditions were documented, we have treated this biomass accumulation (or depletion) term as export production. This choice was made in order to maximize the compatibility of f -ratio-based and pe -ratio-based estimates. Elsewhere, we assumed by necessity that the “steady state” condition is satisfied.

[9] The recorded parameters included mixed layer temperature, depth-integrated chlorophyll, depth-integrated primary production, new production, particle export, depth of the euphotic zone (minimum of the 1% light level or sampling zone), and the carbon-to-chlorophyll ratio (auxiliary material¹ data set text01). The data coverage of our particle export ratio compilation (auxiliary material data set text01) is presented in Figure 1. In general, pe ratios in our data compilation (Figure 1; auxiliary material data set text01) are high (>0.4) in the polar regions, moderate (0.3–0.4) in coastal and those open ocean regions susceptible to phytoplankton blooms, and low (0.05–0.2) elsewhere.

[10] In order to relate the pe ratio to ecosystem size structure, we developed a second compilation using the 39 out of the 122 sites for which such data were available. The recorded parameters included mixed layer temperature, depth-integrated chlorophyll, depth-integrated productivity, euphotic zone depth (1% light level or sampling zone, if less), carbon-to-chlorophyll ratio in phytoplankton, and ecosystem size structure based on a distinction between small (pico- and nano-) and large (micro-) phytoplankton

¹Auxiliary material is available at <ftp://ftp.agu.org/apend/gb/2004GB002390>.

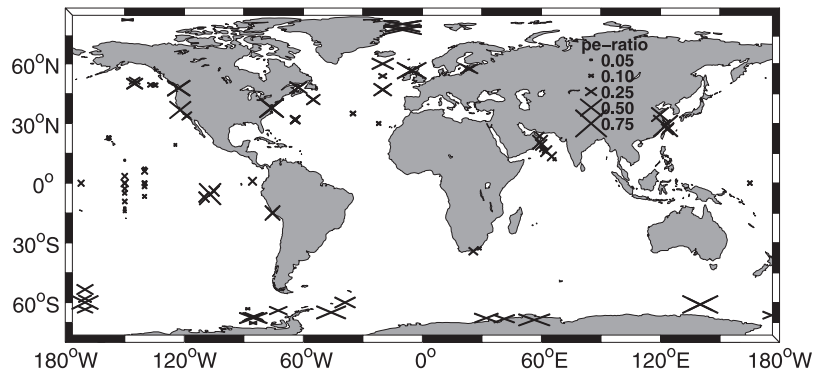


Figure 1. Global map of particle export ratio estimates from the synthesis developed here (auxiliary material data set text01) for calibration of the ecosystem model (equations (2) through (17)) and empirical particle export ratio algorithm (equation (1)). Data are compiled from the following sources: Bacon *et al.* [1996], Barber *et al.* [1996, 2001], Barlow *et al.* [1999], Bender *et al.* [1992, 2000], Bidigare and Ondrusek [1996], Booth and Horner [1997], Boyd and Harrison [1999], Boyd *et al.* [2000], Buesseler *et al.* [1992, 1998, 2003], Bury *et al.* [1995], Carlson *et al.* [1994, 2000], Caron *et al.* [2000], Charette *et al.* [1999], Chavez [1989], Chen *et al.* [2001], Coale *et al.* [1996], Cochlan and Bronk [2001], Cochran *et al.* [1995, 2000], Donald *et al.* [2001], Donali *et al.* [1999], Dugdale *et al.* [1992], Dunne [1999], Dunne *et al.* [2000], Emerson *et al.* [1993, 1997], Eppley *et al.* [1992], Garrison *et al.* [2000], Goericke [1998], Gosselin *et al.* [1997], Hansell *et al.* [1997], Harrison *et al.* [2001], Hiscock *et al.* [2003], Honjo [1996], Jackson and Eldridge [1992], Jochem *et al.* [1993], Joint *et al.* [1993], Karl *et al.* [1996], Knauer *et al.* [1984], Landry *et al.* [1994, 2000], Li and Harrison [2001], Lochte *et al.* [1993], Lorenzen [1968], McCarthy *et al.* [1999], Michaels *et al.* [1994], Moran *et al.* [1997], Murray *et al.* [1989, 1996], Nelson *et al.* [1989], Olli and Heiskanen [1999], Olson *et al.* [2000], Owens *et al.* [1993], Probyn *et al.* [1995], Raimbault *et al.* [1999], Rees *et al.* [1995, 2001], Robins *et al.* [1995], Sambrotto [2001], Sambrotto and Mace [2000], Savidge and Gilpin [1999], Sharp *et al.* [1980], Small *et al.* [1989], Smith and Kemp [2001], Smith [1995], Smith and Nelson [1990], Smith *et al.* [1995, 2000], Steinberg *et al.* [2000], Sweeney *et al.* [2000], Tarran *et al.* [1999], Varela and Harrison [1999], Vezina *et al.* [2000], Waldron *et al.* [1995], Ward *et al.* [1982], Watts and Owens [1999], Welschmeyer and Lorenzen [1985], Welschmeyer *et al.* [1993], Wheeler [1993], Wilkerson and Dugdale [1992], Wilkerson *et al.* [1987, 2000], and Yager *et al.* [1995].

(auxiliary material data set text02). For this last parameter, we used a combination of data on the fraction of production by large (nominally $>5 \mu\text{m}$) phytoplankton, the fraction of phytoplankton biomass in large (nominally $>5 \mu\text{m}$) phytoplankton, and the fraction of grazing on large phytoplankton from mesozooplankton and macrozooplankton where grazing on small phytoplankton was obtained from microzooplankton grazing rates.

3. Results of Empirical Analysis

3.1. Preliminary Statistical Analysis

[11] We first analyzed the particle export data compilation statistically to (1) assess the most significant environmental correlates for particle export and the *pe* ratio, (2) develop a simple empirical algorithm for particle export through the *pe* ratio, and (3) establish a benchmark for assessing the goodness-of-fit for mechanistic models. Our simple parametric linear least squares approach relies on the assumption that the first moment (mean) and the second moment (standard deviation) approximate the underlying variability in the data set. In order for this to be true, the data distribution must have a minimal third moment (skew).

Where a variable distribution's skewness value was many times higher than the Gaussian value (i.e., a few extremely high values controlled the statistical result when a parametric method was applied [Press *et al.*, 1992]), we performed log transformations on the variables before performing statistical tests. For *pe*-ratio estimates, we performed the logit transformation [$\text{logit}(x) = \ln(x/(1-x))$] [Sokal and Rohlf, 1995], which is particularly useful for variables that vary between zero and one and have distributions skewed to the right.

[12] A direct link between primary production and particle export was confirmed in our data compilation, as primary production correlated well with particle export, accounting for 69% of the overall variance (after log transformation of both variables). Furthermore, the slope of the log-log regression from model I (linear least squares with one independent variable) was 1.32, higher than the value of 1.0, suggesting that the primary production data provide additional information on particle export beyond the simple linear dependence (i.e., beyond a constant *pe* ratio). Highly significant ($P < 0.01$) correlations were found between the *pe* ratio and temperature (negative; Figure 2a), log of the chlorophyll concentration (positive; Figure 2b),

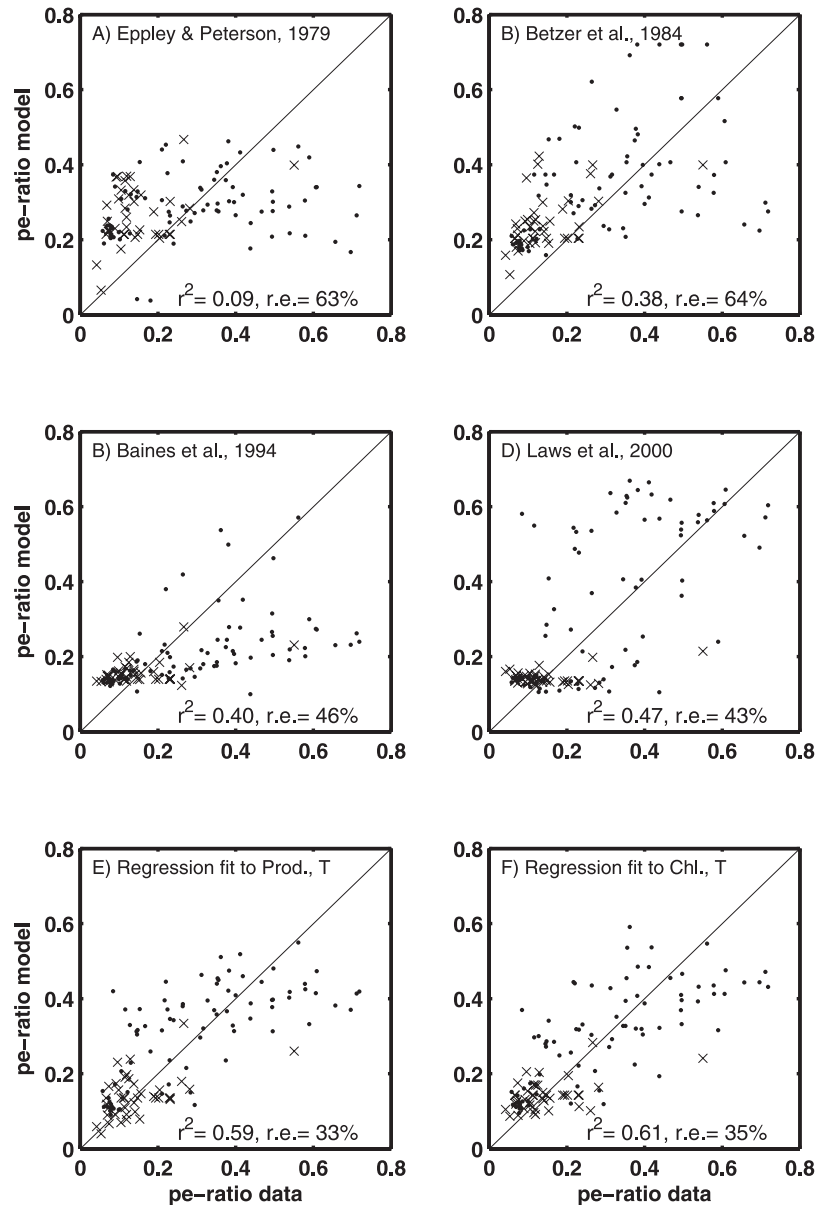


Figure 2. Comparison of particle export ratio estimates of various models with the synthesis in auxiliary material data set text01. The *Eppley and Peterson* [1979] algorithm (empirically derived from their Figure 2 for three regions: (a) $0-140 \text{ gC m}^{-2} \text{ yr}^{-1}$, $ef \text{ ratio} = 0.0025 * \text{Prod}$; $140-500 \text{ gC m}^{-2} \text{ yr}^{-1}$, $pe \text{ ratio} = 0.21 * (\text{Prod} - 140) / \text{Prod} + 0.35$; >500 , $ef \text{ ratio} = 0.5$; where Prod is in units of $\text{gC m}^{-2} \text{ yr}^{-1}$.); (b) the *Betzer et al.* [1984] algorithm ($pe \text{ ratio} = 0.409 * Z_{\text{cu}}^{-0.628} * (\min(\text{Prod}, 228))^{0.41}$; where Prod is in units of $\text{gC m}^{-2} \text{ yr}^{-1}$.); (c) the *Baines et al.* [1994] algorithm ($pe \text{ ratio} = 10^{-0.67 + 0.30 * \log_{10}(\text{Chlinv.}/Z_{\text{cu}})}$); (d) the *Laws et al.* [2000] prognostic relationship taken from the U.S. JGOFS Synthesis and Modeling Project website (<http://usjgofs.whoi.edu/mzweb/syndata.html>). (e) The multilinear regression fit to temperature and volumetric productivity ($pe \text{ ratio} = \max(0.04, \min(0.72, -0.0101 \times T + 0.0582 \times \ln(\text{Prod}/Z_{\text{cu}}) + 0.419))$). (f) The multilinear regression fit to temperature and chlorophyll ($pe \text{ ratio} = \max(0.04, \min(0.72, -0.0081 \times T + 0.0668 \times \ln(\text{Chl}/Z_{\text{cu}}) + 0.426)$); equation (1)). Symbols are grouped by temperature into less than 14°C (crosses) and greater than 14°C (dots).

log of volumetric primary productivity (positive; Figure 2c) and euphotic zone depth (negative; Figure 2d).

[13] In order to assess the sensitivity of our analysis to our choice of pe -ratio versus f -ratio definitions, we went

through an exercise of converting the auxiliary material data set text01 to estimates of f ratio by adding an organic carbon transport fraction to the sinking-based estimates in the same way that the organic carbon transport fraction was

subtracted from the nutrient uptake-based and total export based estimates in the pe -ratio analysis. The resultant similarity in variance (95% based on logit-transformed, squared correlation coefficients) demonstrates the robustness of the analysis with respect to the choice of pe ratio or f ratio as master variable.

3.2. Empirical Models of Particle Export

[14] We establish two empirical, statistical equations for the pe ratio using linear, least squares multiple regression with stepwise addition [Sokal and Rohlf, 1995]. One equation is given in terms of temperature and productivity per unit volume (equation (1a)), and the other in terms of temperature and chlorophyll concentration (equation (1b)),

$$pe_r = -0.0101^\circ\text{C}^{-1} \times T + 0.0582 \times \ln(\text{PP}/Z_{\text{eu}}) + 0.419$$

$$0.04 < pe_r < 0.72 \quad (1a)$$

$$pe_r = -0.0081^\circ\text{C}^{-1} \times T + 0.0668 \times \ln(\text{Chl}/Z_{\text{eu}}) + 0.426$$

$$0.04 < pe_r < 0.72, \quad (1b)$$

where pe_r is pe ratio, temperature (T) is in units of $^\circ\text{C}$, vertically integrated primary production (PP) is in units of $\text{mmol C m}^{-2} \text{d}^{-1}$, the depth of the euphotic zone (Z_{eu}) is in m and vertically integrated chlorophyll (Chl) is in units of mg Chl m^{-3} . The full range of observed pe ratios (0.04–0.72) is provided as lower and upper bounds, in equations (1a) and (1b). We find it particularly interesting that neither regression was significantly improved by the addition of a third term, demonstrating that most of the remaining variance was uncorrelated to the variables included in our data sets.

[15] Comparisons of a variety of empirical parameterizations with the data synthesis are shown in Figure 2. The earliest of these parameterizations, from *Eppley and Peterson* [1979] (Figure 2a), does the least well, accounting for only a small amount (9%) of the variance in the data compilation and having a high relative uncertainty (63%). We attribute this poor fidelity to this parameterization's reliance on the integral of primary production while neglecting temperature and euphotic zone depth. A subsequent parameterization [Betzer *et al.*, 1984] (Figure 2b) that includes both the integral of primary production and euphotic zone depth accounts for a much higher fraction of the variance (38%). However, the relative uncertainty (64%) was not improved. A decade later, *Baines et al.* [1994] (Figure 2c) utilized chlorophyll concentration as a predictive variable. Their parameterization is able account for slightly higher variance (40%) while also decreasing the relative uncertainty (46%). However, this parameterization demonstrates strong bias to low values at higher pe ratios. The *Laws et al.* [2000] (Figure 2d) parameterization, including a sophisticated mechanistic formulation, also succeeds in reproducing the large-scale structure in the data, accounting for nearly half of the variance (47%) and decreasing the relative error (43%). The major shortcoming of the *Laws et al.* [2000] algorithm is its failure to reproduce variability in the pe ratio at high temperatures (dots in

Figure 2b). We suggest that this is due to the *Laws et al.* [2000] choice of weaker temperature dependence for phytoplankton and bacterial metabolism ($\sim e^{0.0633 T}$) than for zooplankton metabolism ($\sim e^{0.1000 T}$), leading to relatively higher efficiency of zooplankton recycling at higher temperatures, such that phytoplankton biomass is maintained at low levels. While the *Laws et al.* [2000] algorithm was originally cast in terms of f ratios, here we apply it to pe ratios. In order to assess the sensitivity of our analysis to this basis choice, we also compared the *Laws et al.* [2000] model to our f -ratio estimates. The *Laws et al.* [2000] model was found to reproduce slightly less variance (42%) when the data synthesis was recast in terms of f ratios rather than pe ratios.

[16] The empirical temperature and productivity regression algorithm developed here (equation (1a) and Figure 2e) fits the data compilation relatively well, reproducing 58% of the variance with a decreased relative uncertainty (33%), but fails to reproduce the areas of highest pe ratio, sites with very high pe ratio and low to moderate primary productivity. Importantly, this problem is ameliorated when biomass instead of productivity is used in the algorithm (equation (1b) and Figure 2f). This formulation also manages to reproduce 61% of the variance and have a relatively low relative error (35%). We suggest that the improvement in reproducing high pe ratios at low temperature using chlorophyll rather than primary production is because biomass integrates ecosystem processes over time to a greater extent than primary production.

[17] A more extensive comparison of empirical parameterizations with the data synthesis is shown in Table 1 in terms of the squared correlation coefficient of each parameterization for particle export and pe ratio, the ratio of logit-transformed pe ratio variances in each model to the data synthesis variance, and the median relative error calculated for each model. The depth dependent parameterization of *Suess* [1980] was found to correlate well with the data, but to severely underestimate the overall variance. The NO_3 -based parameterization of *Platt and Harrison* [1985] was found to have the opposite problem of strongly overestimating the variance. While the primary production-based parameterization of *Wassman* [1990] and the chlorophyll-based parameterization of *Baines et al.* [1994] both underestimate the variance, they significantly improved upon the relative error, bringing it down to 48% and 46%, respectively. Oddly, the biomass-based parameterization of *Legendre* [1998] was able to reproduce the variance of the pe ratio without correlating with the data.

[18] As the uncertainty in any single estimate of the pe ratio is generally no better than 25%, we propose the empirical algorithm (equation (1b)) as a valuable tool for future studies seeking to estimate particle export fluxes using remote sensing. These results suggest that the pe ratio can be described with high accuracy using parameters (temperature and chlorophyll) observable by satellite.

3.3. Intrasite Variability

[19] While the focus of this study is to obtain a global perspective, we also assessed the applicability of the empirical algorithm locally. This is a much more stringent test

Table 1. Squared Regression Coefficients From the Data Compilation in Auxiliary Material Data Set text01 Between Various Parameters and Particle Export and the pe Ratio Along With the Corresponding Data Transformation Performed in Parentheses

Parameter	Input Parameter(s)	r^2 - ln(PE)	r^2 - logit(pe Ratio)	variance Ratio	relative Error, %
Depth of euphotic zone	Z_{eu}	0.31	0.39		
Surface temperature	T	0.18	0.45		
Surface Chl	Chl	0.64 (ln)	0.43 (ln)		
Surface NO_3	NO_3	0.19	0.31		
Primary production	PP	0.74 (ln)	0.28 (ln)		
<i>Eppley and Peterson</i> [1979]	PP	0.69 (ln)	0.09 (logit)	0.24	63
<i>Suess</i> [1980]	Z_{eu}	0.79 (ln)	0.37 (logit)	0.09	59
<i>Betzer et al.</i> [1984]	Z_{eu} , PP	0.81 (ln)	0.38 (logit)	0.44	64
<i>Platt and Harrison</i> [1985]	NO_3	0.70 (ln)	0.42 (logit)	2.48	68
<i>Wassman</i> [1990]	PP	0.78 (ln)	0.26 (logit)	0.36	48
<i>Baines et al.</i> [1994]	Chl	0.80 (ln)	0.40 (logit)	0.21	46
<i>Legendre</i> [1998]	biomass	0.33 (ln)	0.00 (logit)	0.79	79
<i>Laws et al.</i> [2000]	PP, T	0.80 (ln)	0.47 (logit)	0.94	43
Empirical algorithm	PP, T	0.87 (ln)	0.59 (logit)	0.59	35
Empirical algorithm	Chl, T	0.87 (ln)	0.61 (logit)	0.56	35
Mechanistic algorithm	PP	0.85 (ln)	0.55 (logit)	0.35	37
Mechanistic algorithm	biomass	0.80 (ln)	0.42 (logit)	0.35	44
Mechanistic algorithm	PP, T	0.87 (ln)	0.60 (logit)	0.65	33
Mechanistic algorithm	biomass, T	0.87 (ln)	0.61 (logit)	0.61	34

of the algorithm for a variety of reasons: the smaller data sets involved, small dynamic range (variability/uncertainty) and higher uncertainty in the data (due to lack of averaging). This individual site analysis was performed on the six studies for which over 20 data points were available. The resulting correlation coefficients are shown in Table 2. In all six studies, primary production was positively correlated with both biomass and particle export with five of the correlations significant at the 1% level. The correlation between primary production and the pe ratio, however, was negative in five of the six cases, two of which were statistically significant. In general, this result contradicts the large-scale trend seen in the regressions.

[20] A more careful examination of the site analysis shows that our algorithms fail to capture variability primarily at sites where that variability is very low. The standard deviation of the pe ratio at HOT (0.03), BATS (0.04), Line P (0.04) and EqPac (0.05) is small in comparison to the standard deviation across sites (0.18). It is notable that at the Scotland site, where the pe -ratio variability is largest, there is a significant correlation with our algorithms. This suggests that the algorithms are capable of representing large changes in pe ratio (across or within sites), but not small differences in pe ratio at a single site. In the context of

the model of phytoplankton size-structure presented below, this kind of behavior can be expected to be seen when growth rates of small and large phytoplankton vary in a way that is completely decoupled. At nutrient-poor sites such as HOT and BATS, where multiple nutrients may be limiting, such decoupling may be more likely than at sites where there is a strong spring bloom. While the algorithms provide a large-scale estimate of the pe ratio, they do not adequately represent the fine-scale variability of the pe ratio at any particular site, particularly the variability on short temporal and spatial scales (which are smoothed out by the ecosystem when translated to particle export variability) and variability in phytoplankton growth rates (which vary the relationship between biomass, primary production and nutrient utilization).

[21] To put the intrasite variability into an intersite perspective, we also present the standard deviation of pe -ratio values for each site in Table 2. In all cases except for Scotland ($\sigma_{pe\text{-ratio}} = 0.20$), the intrasite standard deviations were much smaller ($\sigma_{pe\text{-ratio}} = 0.03\text{--}0.11$) than the standard deviation of pe ratio across sites for the data synthesis as a whole ($\sigma_{pe\text{-ratio}} = 0.18$; see auxiliary material). While these results demonstrate the limitations of this approach in the lack of sensitivity of the pe -ratio algorithms to small-scale

Table 2. Correlations Between Chlorophyll Biomass, Primary Production, Particle Export, the Particle Export Ratio, the pe Ratio Determined Via Production, the pe Ratio Determined Via Biomass, and Temperature for the Six Sites Listed in Auxiliary Material Data Set text02 for Which a Statistically Large Number of Data Points (>20) was Available^a

Site	Prod: Biomass	Prod: Export	pe Ratio: Prod	pe Ratio: pe Ratio _P	pe Ratio: Biomass	pe Ratio: pe Ratio _B	T: pe Ratio	$\sigma_{pe\text{-ratio}}$	L/P*	n
EqPac	0.93 ^b	0.68 ^b	-0.30	-0.41 ^b	-0.27	-0.32	0.03	0.05	0.2 ± 0.2	24
Arabian Sea	0.79 ^b	0.44 ^b	-0.17	-0.11	-0.01	-0.01	-0.11	0.11	0.6 ± 0.4	36
HOT	0.15	0.20	-0.57 ^b	-0.43 ^b	0.03	0.11	-0.15	0.03	0.14 ± 0.07	94
BATS	0.45 ^b	0.39 ^b	-0.40 ^b	-0.37 ^b	0.12	0.00	0.16	0.04	0.03 ± 0.03	108
Line P	0.36	0.68 ^b	-0.38	-0.38	-0.12	-0.19	0.12	0.04	1.0 ± 0.7	25
Scotland	0.56 ^b	0.94 ^b	0.50 ^b	0.37 ^b	0.43 ^b	0.31	-0.28	0.20	1.5 ± 2.5	39

^aPrimary production, Prod; particle export ratio, pe Ratio; the pe ratio determined via production, pe Ratio_P (equation (1a)); pe ratio determined via biomass, pe Ratio_B (equation (1b)).

^bSignificant correlations at the 95% confidence level.

variability, they are consistent with our goal of obtaining algorithms with global-scale applicability. In the parlance of *Longhurst* [1991], we have described a means of assessing variability in the *pe* ratio between biogeochemical provinces, but not necessarily within them, since most of the observed variability is between biogeochemical provinces.

4. Description of Ecosystem-Based Analysis

4.1. Modeling Phytoplankton Size Structure

[22] Previous work by *Tremblay et al.* [1997] demonstrated empirically that much of the variability in the *f* ratio could be described through variability in ecosystem size structure using a 5- μm distinction between small and large phytoplankton. Recent work by *Agawin et al.* [2000] demonstrated a tight relationship between size structure and concentration wherein large phytoplankton ($>2 \mu\text{m}$ in their study) became an increasing fraction of the biomass as it increased. We interpret this sized-based relationship as resulting from differential grazing of small and large phytoplankton; as primary production and grazing increase, individual biomass in one size class saturates and larger classes of phytoplankton are added to the ecosystem (see *Armstrong* [1999, 2003] for details). The basic assumption is that zooplankton grazing pressure can be expressed implicitly as a function of phytoplankton concentration such that it is able to keep pace with small phytoplankton production while not keeping pace with large phytoplankton production. Specifically, we propose a model with two size classes of phytoplankton, small (S) and large (L), governed by the following equations:

$$\Gamma(S) = \mu_{0S}e^{(kT)}S - \lambda_{0S}e^{(kT)}(S/P^*)S \quad (2a)$$

$$\Gamma(L) = \mu_{0L}e^{(kT)}L - \lambda_{0L}e^{(kT)}(L/P^*)^\alpha L. \quad (2b)$$

In equations (2a) and (2b), Γ is the physical transport and time rate of change operator, μ_{0S} and μ_{0L} are growth rate constants dependent on nutrients and light which we assume to be equal ($\mu_{0S} = \mu_{0L} = \mu_0$; d^{-1}), k is the temperature dependence of growth and loss from *Eppeley* [1972] ($k = 0.063^\circ\text{C}^{-1}$), and λ_{0S} and λ_{0L} are the rate constants of loss, implicitly including the combined effects of grazing, photorespiration, cell death and cell sinking. As with the growth rate constants, we assume the grazing rate constants are equal for small and large plankton ($\lambda_{0S} = \lambda_{0L} = \lambda_0$; d^{-1}). P^* is defined as the pivotal concentration at which S is equal to L ($P^* = S = L$; mmol C m^{-3}). Here α is a scale parameter for the effect of grazing (and other loss terms) on large phytoplankton, and can be thought of conceptually as the degree to which the zooplankton community is unable to adjust to changes in the concentration of large phytoplankton. Assuming that the ecosystem adjusts instantaneously to any changes in forcing and ignoring all physical transport and temporal terms ($\Gamma = 0$), the relationship between the concentration of large and small phytoplankton (equations (2a) and (2b)) becomes

$$(S/P^*) = (L/P^*)^\alpha, \quad (3)$$

and the relationship between primary production (Prod_{tot}) as a function of biomass and temperature becomes

$$\text{Prod}_{\text{tot}} = \mu_0 e^{(kT)}(S + L) = \lambda_0 e^{(kT)}[(S/P^*)S + (L/P^*)^\alpha L]. \quad (4)$$

Three specific choices for the value of α allow for simple analytical solution of size partitioning as a function of biomass or production. These are values of

$$\text{Prod}_{\text{tot}} = \lambda_0 e^{(kT)} P^* \left[(S/P^*)^2 + (S/P^*)^6 \right] \quad \alpha = 1/5, \quad (5a)$$

$$\text{Prod}_{\text{tot}} = \lambda_0 e^{(kT)} P^* \left[(S/P^*)^2 + (S/P^*)^4 \right] \quad \alpha = 1/3, \quad (5b)$$

$$\text{Prod}_{\text{tot}} = \lambda_0 e^{(kT)} P^* \left[(S/P^*)^2 + (S/P^*)^3 \right] \quad \alpha = 1/2. \quad (5c)$$

Equations (5a) and (5c) can be solved using a cubic equation solver [*Press et al.*, 1992] while equation (5b) can be solved using the binomial theorem. Because the two constants λ_0 and P^* only enter into this equation via their product, we can combine them into a single constant, Prod^* , to describe the relationship between primary production and particle export in this model.

$$\text{Prod}^* = \lambda_0 P^*. \quad (6)$$

Mechanistically, Prod^* corresponds to the productivity normalized to $T = 0^\circ\text{C}$ at which productivity by S equals productivity by L. Taking the example case of $\alpha = 1/3$ (which is found below to provide the superior solution) and solving equation (5b) for $(S/P^*)^2$ using the binomial theorem gives

$$(S/P^*)^2 = \left[-1 + \left(1 + 4 * \text{Prod}_{\text{tot}} / (e^{(kT)} \text{Prod}^*) \right)^{1/2} \right] / 2. \quad (7)$$

Equation (7) thus gives us a means of estimating the size composition of the phytoplankton community from primary productivity (Prod_{tot}) and temperature. The fraction of production by large phytoplankton (ϕ_L) and total phytoplankton biomass (P) can then be related to (S/P^*) via equations (5b) and (3),

$$\phi_L = (S/P^*)^2 / \left[1 + (S/P^*)^2 \right] \quad (8)$$

$$P = S + L = P^* \left[(S/P^*) + (L/P^*) \right] = P^* \left[(S/P^*) + (S/P^*)^3 \right]. \quad (9)$$

[23] The power of this method of manipulation of the ecological model is that we have reduced the mechanistic formulation of size structure to two parameters, the rate constant for phytoplankton loss at 0°C (λ_0) and the pivotal concentration at which S is equal to L (P^*), that must be fit

from data. We use these results in developing a model of the link between primary production and particle export.

4.2. Modeling the Impact of Size Structure of the pe Ratio

[24] Given the above model for phytoplankton size structure, we now develop a model to convert that size-resolved primary production into sinking detritus. In addition to the equations above, we require additional equations for detritus (Det), opal (SiO_2) and calcium carbonate (CaCO_3),

$$\begin{aligned} \Gamma(\text{Det}) = & \lambda_0 e^{(kT)} e^{(k_{\text{rem}}T)} ((S/P^*) S \phi_{\text{detS0}} \\ & + (L/P^*)^\alpha L \phi_{\text{detL0}}) - \lambda_{\text{Det}} \max(0, \text{Det}) \\ & - r_D (r_{\text{PSi}} \text{SiO}_2 \text{mw}_{\text{SiO}_2} + r_{\text{PCa}} \text{CaCO}_3 \text{mw}_{\text{CaCO}_3}) \\ & - \partial/\partial z (w \text{Det}), \end{aligned} \quad (10a)$$

$$\Gamma(\text{SiO}_2) = r_{\text{LSi}} \mu_0 e^{(kT)} L - \gamma_{\text{Si}} \text{SiO}_2 - \partial/\partial z (w \text{SiO}_2), \quad (10b)$$

$$\Gamma(\text{CaCO}_3) = r_{\text{LCa}} \mu_0 e^{(kT)} L - \gamma_{\text{Ca}} \text{CaCO}_3 - \partial/\partial z (w \text{CaCO}_3). \quad (10c)$$

[25] Detritus is produced from small and large phytoplankton loss in separate proportions referenced to 0°C (ϕ_{detS0} and ϕ_{detL0} , respectively) with a temperature dependence specified by k_{rem} . Here λ_{Det} is the decay coefficient of detritus and w is the sinking velocity ($w = 100 \text{ m d}^{-1}$; consistent with the compilation of *Allredge and Silver* [1988]). Remineralization of detritus is allowed to occur only above a value protected by mineral SiO_2 and CaCO_3 [*Armstrong et al.*, 2002; *Klaas and Archer*, 2002] with separate ratios of protection of organic material by detritus by opal ($r_{\text{PSi}} = 0.026 \text{ g Organic matter/g SiO}_2$) and calcium carbonate ($r_{\text{PCa}} = 0.070 \text{ g Organic matter/g CaCO}_3$) based on the mass fraction analysis of *Klaas and Archer* [2002], assuming $\text{mw}_{\text{SiO}_2} = 60$ and $\text{mw}_{\text{CaCO}_3} = 100$. Here r_D is a conversion factor between organic mass and nitrogen ($164.1 \text{ g organic matter/mol N}$) based on the work of *Anderson and Sarmiento* [1994].

[26] For the ecosystem model calibration using the pe ratio data compilation (auxiliary material data set text01), observationally based mineral production estimates were not widely available. We assume that silicon and calcium carbonate production is primarily through diatoms and coccolithophorids, which we classify as “large” and make the same steady state assumption as we already have made for the nitrogen cycle. Furthermore, since we are only concerned with the net production of opal and calcium carbonate, we set their dissolution rates to zero within the euphotic zone. Here r_{LSi} and r_{LCa} are conversion factors for mineral production by large phytoplankton in grams of mineral per grams of organic material. Values of $r_{\text{LSi}} = 0.23$ and $r_{\text{LCa}} = 0.23$ were estimated on the basis of the global average ratio of mineral production to primary production, assuming a global SiO_2 production of 7.2 Pg SiO_2 from *Treguer et al.* [1995], a global CaCO_3 production estimate of 7.3 Pg CaCO_3 (average of 5.3 Pg from *Milliman* [1993] and 9.2 Pg from *Lee* [2001]), a global primary

production of 43.5 Pg C [*Behrenfeld and Falkowski*, 1997] and a global fraction of that primary production attributable to large phytoplankton from the full data set in auxiliary material data set text01 ($\phi_L = 0.39$). Finally, we assume that the euphotic zone is well mixed. In this case the equations for silicate and carbonate become

$$\begin{aligned} r_{\text{LSi}} \mu_0 e^{(kT)} L - \gamma_{\text{Si}} \text{SiO}_2 - w \partial \text{SiO}_2 / \partial z \\ = r_{\text{LSi}} \phi_L \text{Prod}_{\text{tot}} w / Z_{\text{eu}} \text{SiO}_2 = 0 \end{aligned} \quad (11a)$$

$$\begin{aligned} r_{\text{LCa}} \mu_0 e^{(kT)} L - \gamma_{\text{Ca}} \text{CaCO}_3 - w \partial \text{CaCO}_3 / \partial z \\ = r_{\text{LCa}} \phi_L \text{Prod}_{\text{tot}} - w / Z_{\text{eu}} \text{CaCO}_3 = 0, \end{aligned} \quad (11b)$$

such that the mineral production becomes directly proportional to large phytoplankton production. Substituting the above mineral measured production term into equation (10) gives the following equation for detritus for a well-mixed euphotic zone:

$$\begin{aligned} e^{(k_{\text{rem}}T)} [\phi_{\text{detS0}} (1 - \phi_L) + \phi_{\text{detL0}} \phi_L] \text{Prod}_{\text{tot}} \\ - \gamma_{\text{Det}} \{ \text{Det} - r_D (r_{\text{PSi}} r_{\text{LSi}} + r_{\text{PCa}} r_{\text{LCa}}) \\ \cdot \text{Prod}_{\text{tot}} \phi_L Z_{\text{eu}} / w \} - w / Z_{\text{eu}} \\ \text{Det} = 0. \end{aligned} \quad (12)$$

We can define the fraction of production that produces detritus protected by mineral $r_B = r_D (r_{\text{PSi}} r_{\text{LSi}} + r_{\text{PCa}} r_{\text{LCa}})$ and the vertically integrated remineralization coefficient ($R = Z_{\text{eu}} \lambda_{\text{Det}} / w$). Since the detritus sinking flux at the base of the euphotic zone is given by $w \text{Det} / Z_{\text{eu}}$, the particle export ratio can then be derived from equation (12) as

$$pe_r = \left[e^{(k_{\text{rem}}T)} \{ \phi_{\text{detS0}} (1 - \phi_L) + \phi_{\text{detL0}} \phi_L \} + R r_B f_L \right] / (1 + R). \quad (13)$$

The power of this method is that once we have partitioned production into large and small phytoplankton fractions, we have reduced the mechanistic formulation of the pe ratio to four parameters to be fit from the data: the remineralization coefficient k_{rem} , the detritus production fractions for small and large phytoplankton ϕ_{detS0} , ϕ_{detL0} and the detritus remineralization rate λ_{Det} .

5. Results of Ecosystem-Based Analysis

5.1. Parameter Estimation for Size Structure

[27] We first consider the estimation of parameters relating to the partitioning of the phytoplankton community into “small” and “large” components, obtaining estimates for Prod^* and α using the data compilation in auxiliary material data set text02. The value of Prod^* was determined by varying Prod^* and computing ϕ_L from primary productivity and temperature observations using equations (7) and (8) so as to minimize the difference between the observed and computed ϕ_L . The data set was resampled 10,000 times with replacement in order to obtain the most likely Prod^* value (the median) and the 95% confidence intervals. This resulted in a value for Prod^* of $0.37 \pm 0.10 \text{ mmol C m}^{-3} \text{ d}^{-1}$, with the fit

accounting for 74% of the variance in the data set with normally distributed residuals. Both our analysis and the previous work of *Agawin et al.* [2000] are consistent with a cubic relationship between small and large phytoplankton (i.e., $\alpha = 1/3$). Values of α higher than $1/3$ (such as $1/2$; equation (5a)) underestimate variability in phytoplankton size composition. Values lower than $1/3$ (such as $1/5$; equation (5c)) fit the data reasonably well but prove to be numerically unstable during forward integration of the L equation (equation (2b); see *May* [1973] for details). Because the data does not strongly constrain the value of α below values of $1/3$, the choice of $\alpha = 1/3$ is somewhat arbitrary from the standpoint of data validation. We chose this particular value primarily because it gives a simple, analytical solution for the phytoplankton size composition as a function of primary production while maximizing the numerical stability of the large phytoplankton equation, important for future implementation of the full ecosystem model.

[28] The pivotal concentration of small and large phytoplankton at which the two are equal, P^* , was obtained iteratively. Observed estimates of biomass were obtained from the chlorophyll inventory and carbon to chlorophyll ratio in auxiliary material data set text01. Model estimates of total phytoplankton biomass were obtained as a function of production and temperature using equations (7) and (9). The optimal value of P^* was found by minimizing the absolute value of $\log(\text{model-data})$ biomass differences. The model-data fit yielded a value of P^* of $1.9 \pm 0.3 \text{ mmol C m}^{-3}$. Assuming a characteristic C:Chl value of 50 g/g [*Fasham et al.*, 1990], this value of P^* correspond to a typical pivotal chlorophyll concentration of $0.5 \text{ mg Chl m}^{-3}$. Substituting this into equation (6) using our optimal value of Prod^* gives $\lambda_0 = 0.19 \pm 0.06 \text{ d}^{-1}$. These parameters (P^* and λ_0) are required for implementation of the fully prognostic ecosystem model in which phytoplankton growth is explicit.

[29] Large-scale consistency of this model with observations of phytoplankton size composition as a function of biomass is evident over the observed range, as shown in Figure 3. At low phytoplankton chlorophyll concentrations, both our data compilation and model-derived estimates diverge from the *Agawin et al.* [2000] data compilation, which has a higher percentage of “large” phytoplankton. This difference is consistent with the difference in size partitioning in the two studies, as *Agawin et al.* [2000] included the nanoplankton (nominally $2\text{--}5 \mu\text{m}$) in the “large” size class with the microplankton (nominally $> 5 \mu\text{m}$), while we include them in the “small” size class with the picoplankton (nominally $< 2 \mu\text{m}$). Additionally, the comparison with the work of *Agawin et al.* [2000] suggests that at low phytoplankton concentrations, the fraction of phytoplankton in the nanoplankton (nominally $2\text{--}5 \mu\text{m}$) range is approximately 30%. For reference, all constants, their definitions, values and sources are given in Table 3.

[30] We also include in Figure 3 a comparison of our model with that of *Denman and Peña* [2002], who propose a simple equation of $\phi_S = P_S/(k_S + P)$. While their derived values of P_S and k_S (dashed line) for the northeast

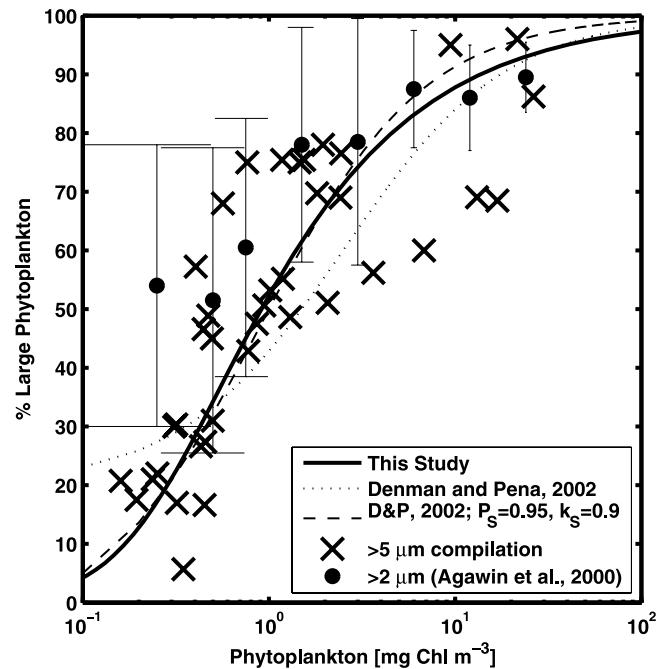


Figure 3. Percentage of large phytoplankton versus the phytoplankton concentration (mg Chl m^{-3}) for: the mechanistic model in this study (equation (3), $\alpha = 1/3$) assuming a constant C:Chl ratio of 50 g/g (solid line), the *Denman and Peña* [2002] equation of $\phi_S = P_S/(k_S + P)$ using their values of $P_S = 2.5 \text{ mg Chl m}^{-3}$ and $k_S = 2.0 \text{ mg Chl m}^{-3}$ (dashed line), the *Denman and Peña* [2002] equation of $\phi_S = P_S/(k_S + P)$ using values to reproduce our result wherein $P_S = 0.95 \text{ mg Chl m}^{-3}$ and $k_S = 0.9 \text{ mg Chl m}^{-3}$ (dotted line), the nominally $> 5 \mu\text{m}$ data synthesis of auxiliary material data set text02 (crosses), and the nominally $> 2 \mu\text{m}$ data synthesis of *Agawin et al.* [2000] (solid circles with error bars indicating 1 standard deviation).

subarctic Pacific Ocean, gave significant biases in phytoplankton size composition at low (where the dashed line is too high) and intermediate (where the dashed line is too low), we were able to ameliorate these deficiencies retuning the values of P_S and k_S to fit this much more extensive data set. Our model is able to reduce the system to four parameters (P^* , λ_0 , k and α) which capture not only the dependence of size structure on temperature and production but also of biomass on temperature and production. We find this result extremely encouraging as it demonstrates that characterization of the primary modes of observed variability does not require a model with many free parameters so long as the model structure is sound. While a similar statement could be made regarding the retuned version of the *Denman and Peña* [2002] algorithm which utilizes only two parameters, we believe that our model presents an improvement in providing the mechanistic underpinning to the observed size relationship: differences in the loss functionalities of small and large phytoplankton. This mechanistic representation is a critical

Table 3. Ecosystem Model Parameters, Their Chosen Value, and the Source

Constant	Definition	Value	Units	Source
μ_0	phytoplankton specific growth rate referenced to $T = 0^\circ\text{C}$	light and nutrient dependent	d^{-1}	not utilized here
k	temperature dependence of growth/grazing	0.063	T^{-1}	<i>Eppley</i> [1972]
k_{rem}	temperature dependence of detritus production	-0.032	T^{-1}	fit using auxiliary material data set text01
λ_0	grazing rate constant referenced to $T = 0^\circ\text{C}$	0.19 ± 0.06	d^{-1}	fit using auxiliary material data set text01
P^*	phytoplankton concentration at which small = large	1.9 ± 0.3	mmol C m^{-3}	fit using auxiliary material data set text01
Prod^*	production referenced to $T = 0^\circ\text{C}$	0.37 ± 0.10	$\text{mmol C m}^{-3} \text{d}^{-1}$	fit using auxiliary material data set text02
α	inverse of the power law relationship between small and large phytoplankton	1/3	none	<i>Agawin et al.</i> [2000]
λ_{Det}	detritus removal rate constant referenced to $T = 0^\circ\text{C}$	0.4	d^{-1}	fit using auxiliary material data set text01
r_{LSi}	SiO_2 production as a fraction of large phytoplankton production	0.23	$\text{mol SiO}_2/\text{mol N}$	<i>Treguer et al.</i> [1995]
r_{LCa}	CaCO_3 production as a fraction of small phytoplankton production	0.23	$\text{mol SiO}_2/\text{mol N}$	<i>Milliman</i> [1993] and <i>Lee</i> [2001]
r_{SiL}	coefficient of organic matter protection for SiO_2	0.026	g organic/g SiO_2	<i>Klaas and Archer</i> [2002]
r_{CaL}	coefficient of organic matter protection for SiO_2	0.070	g organic/g SiO_2	<i>Klaas and Archer</i> [2002]
w	sinking velocity of detritus	100	m d^{-1}	<i>Allredge and Silver</i> [1988]
ϕ_{DetS0}	fraction of large grazing going to detritus referenced to $T = 0^\circ\text{C}$	0.14	none	fit using auxiliary material data set text01
ϕ_{DetL0}	fraction of large grazing going to detritus referenced to $T = 0^\circ\text{C}$	0.74	none	fit using auxiliary material data set text01
r_{D}	organic conversion factor	$12*1.87*117/16$	g organic/mol N	<i>Anderson and Sarmiento</i> [1994]

step toward implementation of the ecosystem model in global general circulation models.

5.2. Parameter Estimation for pe Ratio

[31] We estimate λ_{Det} , k_{rem} , ϕ_{DetS0} and ϕ_{DetL0} using an iterative approach to fit equation (13) to both the observations of *pe* ratio in auxiliary material data set text02 and a regeneration depth scale. The target regeneration depth scale was calibrated against the ‘‘Martin Curve’’ ($F(Z) = F_{\text{Zref}}(Z/Z_{\text{ref}})^{-b}$ [*Martin et al.*, 1987]) as used in the OCMIP II simulations ($Z_{\text{ref}} = 75$ m and $b = 0.9$ [*Najjar and Orr*, 1998]), such that 37% (1/e) of the flux leaving the euphotic zone arrives at 228 m. In the absence of a mineral effect, λ_{Det} would simply be equal to the regeneration depth scale divided by the sinking velocity (w). The inclusion of mineral in the equation, however, implies that the regeneration depth scale for organic matter is a function of the mineral fraction as well as λ_{Det} . We optimized the data fit by iteratively varying λ_{Det} to fit the depth scale of remineralization and then optimizing k_{rem} , ϕ_{DetS0} and ϕ_{DetL0} so as to reproduce the observed *pe* ratios. For a given value of λ_{Det} , values of k_{rem} , ϕ_{DetS0} and ϕ_{DetL0} were obtained by optimizing a maximum likelihood statistic [*Edwards*, 1992; *Hilborn and Mangel*, 1997] based on the logit of the *pe* ratio [$\text{logit}(x) = \ln(x/(1-x))$] through the simulated annealing algorithm [*Metropolis et al.*, 1953; *Press et al.*, 1992] after *Armstrong et al.* [2002]. The λ_{Det} was then recalculated so that the median value of the regeneration depth scale calculated for the 122 individual sites in the data synthesis matched the target value of 228 m. This resulted in optimal values of λ_{Det} , k_{rem} , ϕ_{DetS0} and ϕ_{DetL0} of 0.4 d^{-1} , -0.032,

0.14 and 0.74, respectively. These values of k_{rem} , ϕ_{DetS0} and ϕ_{DetL0} reflect the low export efficiency of the small phytoplankton export pathway at high temperature and high export efficiency of the large phytoplankton export pathway at low temperature.

5.3. Sensitivity of the pe Ratio to Size Structure and Temperature

[32] Equations (7), (8), and (9) provide us with two separate means of estimating ϕ_{L} from data: one by using temperature and primary production in equation (7) and substituting into equation (8), and the second by utilizing biomass data directly. Biomass data can be used by solving equation (9) for S/P^* using a cubic equation solver [*Press et al.*, 1992] and using that value in equation (8). These two formulations of ϕ_{L} can then be substituted into equation (13) to obtain the *pe* ratio in two different ways, one based on primary production and the other on biomass, paralleling the two empirical formulations given in equations (1a) and (1b). In Figure 4, we present four different comparisons between our ecosystem model predictions of the *pe* ratio and the data compilation in auxiliary material data set text01. Results of the parameter fit assuming no temperature dependence in detritus production ($k_{\text{rem}} = 0.0$ in equation (13)) are shown for estimates of ϕ_{L} from primary production and temperature (Figure 4a) and biomass (Figure 4b). While the estimate of ϕ_{L} from primary production and temperature is able to account for a much higher percentage of the variance (55% compared to 42%), it severely underestimates the *pe* ratio at high data values. This result is similar to what was observed in the empirical

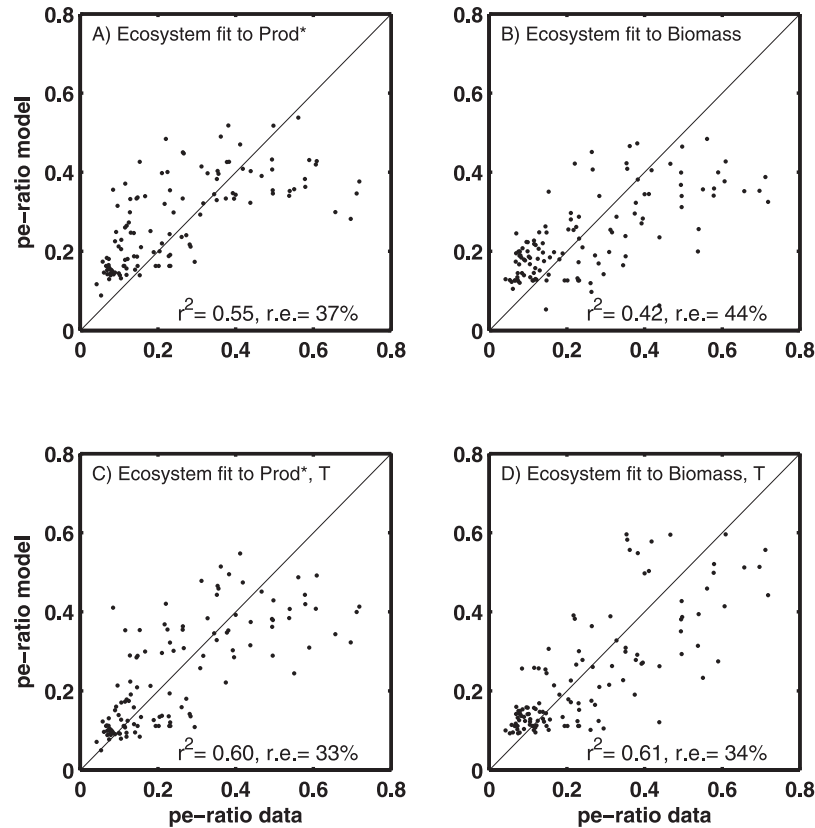


Figure 4. Comparison of particle export ratio estimates from various formulations of the ecosystem model in this study (equations (5) and (8)) with those from the synthesis in auxiliary material data set text01. (a) The ecosystem model fit to $Prod^*$ (productivity at 0°C ; equation (6)) without including a temperature effect on the partitioning to detritus ($k_{rem} = 0.0$) and the ecosystem model fit to $Prod^*$ estimates (productivity at 0°C ; equation (6)) without including a temperature effect on the partitioning to detritus ($\phi_{DetL0} = 0.59$; $\phi_{DetS0} = 0.07$; $k_{rem} = 0.0$). (b) The ecosystem model fit to biomass estimates without including a temperature effect on the partitioning to detritus ($\phi_{DetL0} = 0.52$; $\phi_{DetS0} = 0.05$; $k_{rem} = 0.0$). (c) The ecosystem model fit to $Prod^*$ including a temperature effect on the partitioning to detritus ($\phi_{DetL0} = 0.69$; $\phi_{DetS0} = 0.07$; $k_{rem} = -0.021$). (d) The ecosystem model fit to biomass estimates including a temperature effect on the partitioning to detritus ($\phi_{DetL0} = 0.74$; $\phi_{DetS0} = 0.14$; $k_{rem} = -0.032$).

regression study (Figure 2). Over the seasonal evolution of the spring bloom biomass integrates ecosystem processes over time to a greater extent than primary production. This temporal evolution may explain both the bias in the primary production-based models and higher scatter in the biomass-based models as ecosystems can maintain high biomass after primary productivity has diminished while high biomass is required for high productivity. Incorporating a temperature dependency resulted in a moderate improvement in the primary production-based estimate (Figure 4c) and a vast improvement the biomass-based estimate (Figure 4d). Because of its relative sensitivity and lack of dependence on assumptions for the temperature effect of primary production (k), we consider the biomass-based estimate a much more robust estimate of the temperature dependency on detritus production (k_{rem}). Furthermore, the biomass and temperature based estimate was able to reproduce the highest overall percentage of the variance (61%). A summary comparison of squared regression coefficients

for particle export and the pe ratio for the mechanistic model configurations is included in Table 1.

6. Discussion

[33] The ecosystem model described above is able to reproduce observed variability in ecosystem size structure (Figure 3) and the pe ratio (Figure 4) while retaining a high degree of mathematical simplicity facilitating broad calibration by field observations. It provides a simple mechanistic explanation for both of the empirical size-structure relationships previously observed by *Tremblay et al.* [1997] and *Agawin et al.* [2000]. The detritus regeneration mechanism used in this study, first-order regeneration of unprotected detritus and no remineralization of protected detritus, has the advantage of being mechanistically applicable to both the ocean surface and its interior. This frees us from having to invoke an additional interior remineralization algorithm (e.g., the empirical power law of *Martin et al.* [1987]) or

include multiple detritus components in order to have a portion of detritus remineralization occurring at great depths.

6.1. Sensitivity of pe Ratio to Recycling Formulation

[34] While consistent with the theory of plankton community succession [e.g., *Armstrong*, 1999, 2003], this powerful yet simple approach comes at the cost of a fixed power law to represent the ratio of phytoplankton loss processes (equations (2a) and (2b)). Furthermore, analytical solution of the simple power relation between large and small phytoplankton requires that each have only a single loss term. This prohibits the incorporation of an explicit separation between grazing, mortality, aggregation and other terms in the functionality of phytoplankton loss. The detritus formulation, however, does not fall under this constraint. This flexibility afforded us the opportunity to test the impact of different functionalities of detritus formulation on particle export. One sensitivity test involved the incorporation of an extra term for large phytoplankton concentration in the detritus production formulation to simulate aggregation as a necessary step in detritus formation (i.e., $\phi_{\text{det},L0}$ becomes a function of L). This and other altered configurations had a negligible effect on the model fit, improving our confidence in the model. Indeed, the estimated fraction of detritus protected from remineralization is quite small within the euphotic zone, ranging from 4 to 8%, making euphotic zone model calibration insensitive to this component.

[35] When the mechanistic model is applied using biomass as an input, the temperature input has only one role: limiting detritus production through the $e^{k_{\text{rem}}T}$ term in equation (10a). When the mechanistic model is applied using primary production as an input, however, temperature has two additional roles: modulating both phytoplankton growth and loss through the e^{kT} term in equations (2a) and (2b). Applying the mechanistic model with biomass as an input thus allows us to study the first term (effect of temperature on detritus production) in isolation. We were very encouraged that both methods resulted in the same value of the coefficient for this temperature effect (k_{rem}). It is unclear, however, why detritus production should depend on temperature. Possible explanations include such direct mechanisms as (1) differing temperature coefficients for phytoplankton growth and zooplankton grazing [e.g., *Laws et al.*, 2000], (2) variability in the temperature coefficients for growth within the phytoplankton species assemblage [e.g., *Longhurst*, 1991], (3) variability in the temperature coefficients for grazing within the zooplankton species assemblage [e.g., *Longhurst*, 1991], (4) temperature dependence in particle stickiness [*Allredge et al.*, 1995], (5) temperature dependence in transparent exopolymer production rates [*Passow et al.*, 1995], and (6) temperature dependence in transparent exopolymer destruction rates through variability in bacterial growth rates [*Smith et al.*, 1992]. Potential indirect mechanisms also exist, including (1) the relationship between water column stability and temperature leading to variable light limitation [*Sverdrup*, 1953; *Legendre and Rassoulzadegan*, 1996], and (2) temporal variability in light limitation toward the poles and subsequent decou-

pling between growth and grazing [*Evans and Parslow*, 1985; *Legendre and Rassoulzadegan*, 1996]. Unfortunately, we cannot distinguish between these competing potential mechanisms at this time, though all are deserving of further study.

6.2. Limitations of This Approach With Respect to Stable Ecosystems

[36] In the discussion of the empirical algorithms, we demonstrated a general lack of fidelity in reproducing intrasite variability for the few sites for which large sample sizes are available (Table 2). The relative insensitivity of this approach to intrasite variability can be explained in the context of the mechanistic model as resulting from a general lack of ecosystem size structure variability. Modeled ecosystem size structure is indicated by the variable L/P^* , shown in average and standard deviation for each site in Table 2. When this variable is equal to 1.0, the ecosystem is modeled to be composed of equal fractions of large and small phytoplankton. Variability about this value will effect large changes in the modeled pe ratio. With the small values of L/P^* at EqPac, HOT and BATS, and to a lesser extent the Arabian Sea, the small size class is always dominant, so the model does not predict large changes in the pe ratio. The broad-scale relationship between pe ratio and phytoplankton size composition is borne out at the Scotland site, however, where the model demonstrated significant skill over a large range of L/P^* .

6.3. What Controls Variability in Particle Export From the Surface Ocean?

[37] Analysis of the empirical and mechanistic models developed here allows us to shed new light on the question: What controls variability in particle export from the surface ocean? While the proximate control on particle sinking is the presence of biomass capable of sinking, the ultimate control is the capability to produce biomass. We can thus explore the particle export question by evaluating two alternate hypotheses: control by particle production versus control by particle sinking. The strong correlation between primary production and particle export that accounted for 74% of the variance (Table 1) is suggestive that variability in particle export is dominated by the ability to produce particles through primary production (ultimate control). While such a correlation has been observed many times previously [e.g., *Eppley and Peterson*, 1979], its dominance as the leading-order term is an important statistical justification for an interpretation of particle export by normalizing it to primary production (i.e., using pe ratios). Our mechanistic model demonstrates that variability in the pe ratio can be explained in terms of a simple representation of ecosystem size structure that can be predicted as a function of a pivotal biomass concentration dividing ecosystems dominated by small and large phytoplankton, each with vastly different export efficiencies. Because the fraction of phytoplankton with high export efficiencies increases with increasing primary productivity, pe ratio increases with primary productivity. We can separate these effects using the mechanistic model, as primary productivity by small phytoplankton alone (equations (7) and (8)) accounts for

only 59% of the variability in particle export. This result implies that the covariance of productivity and phytoplankton size structure explains the rest of the correlation between primary productivity and particle export. As the full mechanistic model accounted for 87% of the variance in particle export, proximate control (through phytoplankton size composition and temperature) accounts for 28% of this. Thus we conclude that particle export variability is regulated by a combination of: ultimate control by particle production (accounting for a majority 59%) and proximate control by the ability to create sinking material through phytoplankton size composition and temperature (accounting for a minority 28%). We are unable to explain 13% of the particle export variability. While much of this unexplained variance may be due to observational uncertainty, some of it is due to other, unresolved controls such as those discussed above with respect to intrasite variability.

7. Conclusions

[38] We synthesized observations of the particle export ratio to calibrate empirical algorithms of the particle export ratio as a function of biomass (or productivity) and temperature. We also developed a mechanistic, ecosystem-based model of the particle export ratio (*pe* ratio) which depends on biomass (or productivity) and temperature. In developing a model of phytoplankton size structure, export efficiency and mineral protection of sinking detritus, we thus combine the empirical results of Tremblay *et al.* [1997], Agawin *et al.* [2000], Armstrong *et al.* [2002] and Klaas and Archer [2002] into an internally consistent, mechanistic framework. The model is driven by the differing loss terms and export efficiencies of large phytoplankton (where loss is proportional to the four-thirds power of biomass and efficiently exported) and small phytoplankton (where loss is proportional to the second power of biomass and inefficiently exported). We demonstrate that both the empirical regression and the simple ecosystem size-based model reproduce the observed variability in *pe* ratios. The mechanistic model achieves this skill through the separation of the temporally stable microbial loop involving small phytoplankton, which are efficiently recycled and vary little in biomass, from the relative boom-and-bust ecology involving larger, mineral-forming phytoplankton that provide sinking material, are not recycled efficiently, and vary considerably in biomass. In addition, we demonstrate a small but robust temperature effect on the efficiency of detritus production.

[39] In its ability to represent a high degree of *pe*-ratio variability with a minimum number of free parameters, the biological scheme that we have developed here is a powerful alternative to complex ecosystem models. The simple size-based formulation of phytoplankton loss in equations (2a) and (2b) proves to be a powerful means of describing phytoplankton community composition (Figure 3) while the temperature and size dependent detritus production formulation (equations (10a)–(10c)) is able to transfer this information into a successful description of *pe*-ratio variability (equation (13) and Figure 4). The formulation of mineral protection of detritus (equations (10a)–(10c)) allows us to apply this model to the full water column, rather than just the

surface. Combined, these three ecosystem formulations provide us with a powerful new tool for understanding global biogeochemical cycles that is simple and testable.

[40] **Acknowledgments.** This research was supported by the Department of Energy Office of Biological and Environmental Research under the Ocean Carbon Sequestration Initiative (DOE grant DE-FG0200ER63009), the Carbon Modeling Consortium (NOAA grant NA56GP0439), and the NOAA Geophysical Fluid Dynamics Laboratory. We thank the many people who provided comments and critical reviews to improve the manuscript.

References

- Agawin, N. S. R., C. M. Duarte, and S. Agustí (2000), Nutrient and temperature control of the contribution of picoplankton to phytoplankton biomass and production, *Limnol. Oceanogr.*, *45*, 591–600.
- Aksnes, D. L., and P. Wassmann (1993), Modeling the significance of zooplankton grazing for export production, *Limnol. Oceanogr.*, *38*, 978–985.
- Allredge, A. L., and M. W. Silver (1988), Characteristics, dynamics and significance of marine snow, *Prog. Oceanogr.*, *20*, 41–82.
- Allredge, A. L., C. Gotschalk, U. Passow, and U. Riebesell (1995), Aggregation of a diatom bloom in a mesocosm: Bulk and individual particle optical measurements, *Deep Sea Res., Part II*, *6*, 9–27.
- Anderson, L. A., and J. L. Sarmiento (1994), Redfield ratios of remineralization determined by nutrient data-analysis, *Global Biogeochem. Cycles*, *8*, 65–80.
- Armstrong, R. A. (1999), Stable model structures for representing biogeochemical diversity and size spectra in plankton communities, *J. Plankton Res.*, *21*, 445–464.
- Armstrong, R. A. (2003), A hybrid spectral representation of phytoplankton growth and zooplankton response: The “control rod” model of plankton interaction, *Deep Sea Res., Part II*, *50*, 2895–2916.
- Armstrong, R. A., C. Lee, J. I. Hedges, S. Honjo, and S. G. Wakeham (2002), A new, mechanistic model for organic carbon fluxes in the ocean based on the quantitative association of POC with ballast minerals, *Deep Sea Res., Part II*, *49*, 219–236.
- Aufdenkampe, A. K., J. J. McCarthy, J. P. Dunne, M. Rodier, C. Navarette, and J. W. Murray (2001), Estimation of new production in the tropical Pacific, *Global Biogeochemical Cycles*, *15*, 101–113.
- Bacon, M. P., J. K. Cochran, D. Hirshberg, T. R. Hammar, and A. P. Fleer (1996), Export fluxes of carbon at the equator during the EqPac time-series cruises estimated from ²³⁴Th measurements, *Deep Sea Res., Part II*, *43*, 1133–1154.
- Baines, S. B., M. L. Pace, and D. M. Karl (1994), Why does the relationship between sinking flux and planktonic primary production differ between lakes and oceans?, *Limnol. Oceanogr.*, *39*, 213–226.
- Barber, R. T., M. P. Sanderson, S. T. Lindley, F. Chai, J. Newton, C. C. Trees, D. G. Foley, and F. P. Chavez (1996), Primary productivity and its regulation in the equatorial Pacific during and following the 1991–1992 El Niño, *Deep Sea Res., Part II*, *43*, 933–969.
- Barber, R. T., J. Marra, R. C. Bidigare, L. A. Codispoti, D. Halpern, Z. Johnson, M. Latasa, R. Goericke, and S. L. Smith (2001), Primary productivity and its regulation in the Arabian Sea during 1995, *Deep Sea Res., Part II*, *48*, 1127–1172.
- Barlow, R. G., R. F. C. Mantoura, and D. G. Cummings (1999), Monsoonal influence on the distribution of phytoplankton pigments in the Arabian Sea, *Deep Sea Res., Part II*, *46*, 677–699.
- Behrenfeld, M. J., and P. G. Falkowski (1997), Photosynthetic rates derived from satellite-based chlorophyll concentration, *Limnol. Oceanogr.*, *42*, 1–20.
- Bender, M. L., H. Ducklow, J. Kiddon, J. Marra, and J. Martin (1992), The carbon balance during the 1989 spring bloom in the North Atlantic Ocean, *47N*, *20W*, *Deep Sea Res.*, *39*, 1707–1725.
- Bender, M. L., M.-L. Dickson, and J. Orchoardo (2000), Net and gross production in the Ross Sea as determined by incubation experiments and dissolved O₂ studies, *Deep Sea Res., Part II*, *47*, 3141–3158.
- Betzer, P. R., W. J. Showers, E. A. Laws, C. D. Winn, G. R. DiTullio, and P. M. Kroopnick (1984), Primary productivity and particle fluxes on a transect of the equator at 153W in the Pacific Ocean, *Deep Sea Res.*, *31*, 1–11.
- Bidigare, R. R., and M. E. Ondrusek (1996), Spatial and temporal variability of phytoplankton pigment distributions in the central equatorial Pacific Ocean, *Deep Sea Res., Part II*, *43*, 809–834.
- Bishop, J. K. B. (1989), Regional extremes in particulate matter composition and flux: Effects on the chemistry of the ocean interior, in *Produc-*

- tivity of the Ocean: Present and Past, edited by W. H. Berger, V. S. Smetacek, and G. Wefer, pp. 117–137, John Wiley, Hoboken, N. J.
- Booth, B. C., and R. A. Horner (1997), Microalgae on the Arctic Ocean Section, 194: Species abundance and biomass, *Deep Sea Res., Part II*, 44, 1607–1622.
- Boyd, P., and P. J. Harrison (1999), Phytoplankton dynamics in the NE subarctic Pacific, *Deep Sea Res., Part II*, 46, 2405–2432.
- Boyd, P., et al. (2000), A mesoscale phytoplankton bloom in the polar Southern Ocean stimulated by iron fertilization, *Nature*, 407, 695–702.
- Buesseler, K. O., M. Bacon, J. K. Cochran, and H. Livingston (1992), Carbon and nitrogen export during the JGOFS North Atlantic Bloom Experiment estimated from ^{234}Th : ^{238}U disequilibria, *Deep Sea Res.*, 39, 1115–1137.
- Buesseler, K., L. Ball, J. Andrews, C. Benitez-Nelson, R. Belostock, F. Chai, and Y. Chao (1998), Upper ocean export of particulate organic carbon in the Arabian Sea derived from thorium-234, *Deep Sea Res., Part II*, 44, 2461–2487.
- Buesseler, K. O., R. T. Barber, M.-L. Dickson, M. R. Hiscock, J. K. Moore, and R. Sambrotto (2003), The effect of marginal ice-edge dynamics on production and export in the Southern Ocean along 170°W, *Deep Sea Res., Part II*, 50, 579–603.
- Bury, S. J., N. J. P. Owens, and T. Preston (1995), ^{13}C and ^{15}N uptake by phytoplankton in the Bellinghousen Sea, Austral spring 1992, *Deep Sea Res., Part II*, 42, 1225–1252.
- Carlson, C. A., H. W. Ducklow, and A. F. Michaels (1994), Annual flux of dissolved organic carbon from the euphotic zone in the northwestern Sargasso Sea, *Nature*, 371, 405–408.
- Carlson, C. A., D. A. Hansell, E. T. Peltzer, and W. O. Smith Jr. (2000), Stocks and dynamics of dissolved and particulate organic matter in the southern Ross Sea, Antarctica, *Deep Sea Res., Part II*, 47, 3201–3225.
- Caron, D. A., M. R. Dennett, D. J. Lonsdale, D. M. Moran, and L. Shalapyonok (2000), Microzooplankton herbivory in the Ross Sea, Antarctica, *Deep Sea Res., Part II*, 47, 3249–3272.
- Charette, M. A., S. B. Moran, and J. K. B. Bishop (1999), ^{234}Th as a tracer of particulate organic carbon export in the subarctic northeast Pacific Ocean, *Deep Sea Res., Part II*, 46, 2833–2861.
- Chavez, F. P. (1989), Size distribution of phytoplankton in the central and eastern tropical Pacific, *Global Biogeochem. Cycles*, 3, 27–35.
- Chen, Y. L., H.-Y. Chen, W.-H. Lee, C.-C. Hun, G. T. F. Wong, and J. Kanda (2001), New production in the East China Sea, comparison between well-mixed winter and stratified summer conditions, *Cont. Shelf. Res.*, 21, 751–764.
- Coale, K. H., et al. (1996), A massive phytoplankton bloom induced by an ecosystem-scale iron fertilization experiment in the equatorial Pacific, *Nature*, 383, 495–501.
- Cochlan, W. P., and D. A. Bronk (2001), Nitrogen uptake kinetics in the Ross Sea, Antarctica, *Deep Sea Res., Part II*, 48, 4127–4153.
- Cochran, J. K., C. Barnes, D. Achman, and D. J. Hirshberg (1995), Thorium-234/Uranium-238 disequilibrium as an indicator of scavenging rates and particulate organic carbon fluxes in the Northeast Water Polyna, Greenland, *J. Geophys. Res.*, 100(C3), 4399–4410.
- Cochran, J. K., K. O. Buesseler, M. P. Bacon, H. W. Wang, D. J. Hirschberg, L. Ball, J. Andrews, G. Crossin, and A. Fler (2000), Short-lived isotopes (^{234}Th , ^{228}Th) as indicators of POC export and particle cycling in the Ross Sea, Southern Ocean, *Deep Sea Res., Part II*, 47, 3451–3490.
- Denman, K. L., and M. A. Peña (2002), The response of two coupled one-dimensional mixed layer/planktonic ecosystem models to climate change in the NE subarctic Pacific Ocean, *Deep Sea Res., Part II*, 49, 5739–5757.
- Donald, K. M., I. Joint, A. P. Rees, E. M. S. Woodward, and G. Savidge (2001), Uptake of carbon, nitrogen and phosphorus by phytoplankton along the 20W meridian in the NE Atlantic between 57.5N and 37N, *Deep Sea Res., Part II*, 48, 873–897.
- Donali, E., K. Olli, A.-S. Heiskanen, and T. Andersen (1999), Carbon flows in the planktonic food web of the Gulf of Riga, the Baltic Sea: A reconstruction by the inverse method, *J. Mar. Syst.*, 23, 251–268.
- Dugdale, R. G., and J. J. Goering (1967), Uptake of new and regenerated forms of nitrogen in primary productivity, *Limnol. Oceanogr.*, 23, 196–206.
- Dugdale, R. C., F. P. Wilkerson, R. T. Barber, and F. P. Chavez (1992), Estimating new production in the equatorial Pacific Ocean at 150W, *J. Geophys. Res.*, 97(C1), 681–686.
- Dunne, J. P. (1999), Measured and modeled particle export in equatorial and coastal upwelling regions, Ph. D. thesis, 167 pp., Univ. of Washington, Seattle.
- Dunne, J. P., J. W. Murray, M. Rodier, and D. A. Hansell (2000), Export flux in the western and central equatorial Pacific: Zonal and temporal variability, *Deep Sea Res., Part I*, 47, 901–936.
- Edwards, A. W. F. (1992), *Likelihood*, Johns Hopkins Univ. Press, Baltimore, Md.
- Emerson, S., P. Quay, and P. A. Wheeler (1993), Biological productivity determined from oxygen mass balance and incubation experiments, *Deep Sea Res., Part I*, 40, 2351–2358.
- Emerson, S., P. Quay, D. Karl, C. Winn, L. Tupas, and M. Landry (1997), Experimental determination of organic carbon flux from open-ocean waters, *Nature*, 389, 951–954.
- Eppley, R. W. (1972), Temperature and phytoplankton growth in the sea, *Fish. Bull.*, 70, 1063–1085.
- Eppley, R. W., and B. J. Peterson (1979), Particulate organic matter flux and planktonic new production in the deep ocean, *Nature*, 282, 677–680.
- Eppley, R. W., F. P. Chavez, and R. T. Barber (1992), Standing stocks of particulate carbon and nitrogen in the equatorial Pacific at 150°W, *J. Geophys. Res.*, 97(C1), 655–661.
- Evans, G. T., and J. S. Parslow (1985), A model of annual plankton cycles, *Biol. Oceanogr.*, 3, 327–347.
- Fasham, M. J. R., H. W. Ducklow, and S. M. McKelvie (1990), A nitrogen-based model of plankton dynamics in the oceanic mixed layer, *J. Mar. Res.*, 48, 591–639.
- Garrison, D. L., et al. (2000), Microbial food web structure in the Arabian Sea: A U.S. JGOFS study, *Deep Sea Res., Part II*, 47, 1387–1422.
- Goericke, R. (1998), Response of phytoplankton community structure and taxon-specific growth rates to seasonally varying physical forcing in the Sargasso Sea off Bermuda, *Limnol. Oceanogr.*, 43, 921–935.
- Gosselin, M., M. Levasseur, P. A. Wheeler, R. A. Horner, and B. C. Booth (1997), New measurements of phytoplankton and ice algal production in the Arctic Ocean, *Deep Sea Res., Part II*, 44, 1623–1944.
- Hansell, D. A., C. A. Carlson, N. A. Bates, and A. Poisson (1997), Horizontal and vertical removal of organic carbon in the equatorial Pacific Ocean: A mass balance assessment, *Deep Sea Res., Part II*, 44, 2115–2130.
- Harrison, W. G., T. Platt, and M. R. Lewis (1987), F-ratio and its relationship to ambient nutrient concentration in coastal waters, *J. Plankton Res.*, 9, 225–248.
- Harrison, W. G., J. Aristegui, E. J. H. Head, W. K. W. Li, A. R. Longhurst, and D. D. Sameoto (2001), Basin-scale variability in plankton biomass and community metabolism in the sub-tropical North Atlantic Ocean, *Deep Sea Res., Part II*, 48, 2241–2269.
- Hilborn, R., and M. Mangel (1997), *The Ecological Detective: Confronting Models with Data*, Princeton Univ. Press, Princeton, N. J.
- Hiscock, M. R., J. Marra, W. O. Smith Jr., R. Goericke, C. Measures, S. Vink, R. J. Olson, H. M. Sosik, and R. T. Barber (2003), Primary productivity and its regulation in the Pacific Sector of the Southern Ocean, *Deep Sea Res., Part II*, 50, 533–558.
- Honjo, S. (1996), Fluxes of particles to the interior of the open oceans, in *SCOPE 57: Particle Flux in the Ocean*, edited by V. Ittekkot et al., pp. 91–254, John Wiley, Hoboken, N. J.
- Jackson, G. A., and P. E. Eldridge (1992), Food web analysis of a planktonic system off Southern California, *Prog. Oceanogr.*, 30, 223–251.
- Jochem, F. J., F. Pollehne, and B. Zeitzschel (1993), Productivity regime and phytoplankton size structure in the Arabian Sea, *Deep Sea Res., Part II*, 40, 711–735.
- Joint, I., A. Pomeroy, G. Savidge, and J. W. Wood (1993), Size-fractionated primary productivity in the northeast Atlantic in May–July 1989, *Deep Sea Res., Part II*, 40, 423–440.
- Karl, D. M., J. R. Christian, J. E. Dore, D. V. Hebel, R. M. Letelier, L. M. Tupas, and C. D. Winn (1996), Seasonal and interannual variability in primary production and particle flux at station ALOHA, *Deep Sea Res., Part II*, 43, 539–568.
- Klaas, C., and D. E. Archer (2002), Association of sinking organic matter with various types of mineral ballast in the deep sea: Implications for the rain ratio, *Global Biogeochem. Cycles*, 16(4), 1116, doi:10.1029/2001GB001765.
- Knauer, G. A., J. H. Martin, and D. M. Karl (1984), The flux of particulate organic matter out of the euphotic zone, in *Global Ocean Flux Studies: Proceedings of a Workshop*, pp. 136–150, Natl. Acad. Press, Washington, D. C.
- Landry, M. R., C. J. Lorenzen, and W. K. Peterson (1994), Mesozooplankton grazing in the Southern California Bight: II. Grazing impact and particulate flux, *Mar. Ecol. Prog. Ser.*, 115, 73–85.
- Landry, M. R., J. Constantinou, M. Latasa, S. L. Brown, R. R. Bidigare, and M. E. Ondrusek (2000), Biological response to iron fertilization in the eastern equatorial Pacific (IronEx II): III. Dynamics of phytoplankton growth and microplankton grazing, *Mar. Ecol. Prog. Ser.*, 201, 57–72.
- Laws, E. A., P. G. Falkowski, W. O. Smith, H. Ducklow, and J. J. McCarthy (2000), Temperature effects on export production in the open ocean, *Global Biogeochem. Cycles*, 14, 1231–1246.

- Lee, K. (2001), Global net community production estimated from the annual cycle of surface water total dissolved inorganic carbon, *Limnol. Oceanogr.*, **46**, 1287–1297.
- Legendre, L. (1998), Flux of particulate organic material from the euphotic zone of oceans: Estimation from phytoplankton biomass, *J. Geophys. Res.*, **103**(C2), 2897–2903.
- Legendre, L., and F. Rassoulzadegan (1996), Food-web mediated export of biogenic carbon in oceans: Hydrodynamic control, *Mar. Ecol. Prog. Ser.*, **145**, 179–193.
- Li, W. K. W., and W. G. Harrison (2001), Chlorophyll, bacteria and picoplankton in ecological provinces of the North Atlantic, *Deep Sea Res., Part II*, **48**, 2271–2293.
- Lochte, K., H. W. Ducklow, M. J. R. Fasham, and C. Steinen (1993), Plankton succession and carbon cycling at 47N 20W during the JGOFS North Atlantic Bloom Experiment, *Deep Sea Res., Part II*, **40**, 91–114.
- Longhurst, A. R. (1991), Role of the marine biosphere in the global carbon cycle, *Limnol. Oceanogr.*, **36**, 1507–1526.
- Lorenzen, C. J. (1968), Carbon/chlorophyll relationships in an upwelling area, *Limnol. Oceanogr.*, **14**, 735–745.
- Martin, J. H., G. A. Knauer, D. M. Karl, and W. W. Broenkow (1987), VERTEX—Carbon cycling in the northeastern Pacific, *Deep Sea Res., Part I*, **34**, 267–285.
- May, R. M. (1973), *Stability and Complexity in Model Ecosystems*, Princeton Univ. Press, Princeton, N. J.
- McCarthy, J. J., C. Garside, and J. L. Nevins (1999), Nitrogen dynamics during the Arabian Sea Northeast Monsoon, *Deep Sea Res., Part II*, **46**, 1623–1664.
- Metropolis, N., A. W. Rosenbluth, M. N. Rosenbluth, A. H. Teller, and E. Teller (1953), Equation of state calculations by fast computing machines, *J. Chem. Phys.*, **21**, 1087–1092.
- Michaels, A. F., N. R. Bates, K. O. Buesseler, C. A. Carlson, and A. H. Knap (1994), Carbon system imbalances in the Sargasso Sea, *Nature*, **372**, 537–540.
- Milliman, J. D. (1993), Production and accumulation of calcium carbonate in the ocean: Budget of a nonsteady state, *Global Biogeochem. Cycles*, **7**, 927–957.
- Moran, S. B., K. M. Ellis, and J. N. Smith (1997), $^{234}\text{Th}/^{238}\text{U}$ disequilibrium in the central Arctic Ocean: Implications for particulate organic carbon export, *Deep Sea Res., Part II*, **44**, 1593–1606.
- Murray, J. W., J. Downs, S. Strom, C.-L. Wei, and H. W. Jannasch (1989), Nutrient assimilation, export production and ^{234}Th scavenging in the eastern equatorial Pacific, *Deep Sea Res.*, **36**, 1471–1489.
- Murray, J. W., J. Young, J. Newton, J. Dunne, T. Chapin, B. Paul, and J. J. McCarthy (1996), Export flux of particulate organic carbon from the central equatorial Pacific determined using a combined drifting trap- ^{234}Th approach, *Deep Sea Res., Part II*, **43**, 1095–1132.
- Najjar, R., and J. C. Orr (1998), Design of OCMIP-2 simulations of chlorofluorocarbons, the solubility pump and common biogeochemistry, internal OCMIP report, 25 pp., Lab. des Sci. du Clim. et de l'Environ., *Comm. à l'Energie Atom.*, Gif-sur-Yvette, France.
- Nelson, D. M., W. O. Smith Jr., R. D. Muench, L. I. Gordon, C. W. Sullivan, and D. M. Husby (1989), Particulate matter and nutrient distributions in the ice-edge zone of the Weddell Sea: Relationship to hydrography during late summer, *Deep Sea Res.*, **36**, 191–209.
- Olli, K., and A.-S. Heiskanen (1999), Seasonal stages of phytoplankton community structure and sinking loss in the Gulf of Riga, *J. Mar. Syst.*, **23**, 165–184.
- Olson, R. J., H. M. Sosik, A. M. Chekalyuk, and A. Shalapyonok (2000), Effects of iron enrichment on phytoplankton in the Southern Ocean during late summer: Active fluorescence and flow cytometric analyses, *Deep Sea Res., Part II*, **47**, 3181–3200.
- Owens, N. J. P., P. H. Burkill, R. F. C. Mantoura, E. M. S. Woodward, I. E. Bellan, J. Aiken, R. J. M. Howland, and C. A. Llewellyn (1993), Size-fractionated primary production and nitrogen assimilation in the north-western Indian Ocean, *Deep Sea Res., Part II*, **40**, 697–709.
- Pace, M. L., G. A. Knauer, D. M. Karl, and J. H. Martin (1987), Primary production, new production and vertical flux in the eastern Pacific Ocean, *Nature*, **325**, 803–804.
- Passow, U., A. L. Alldredge, and B. E. Logan (1995), The role of articulate carbohydrate exudates in the flocculation of diatom blooms, *Deep Sea Res., Part I*, **41**, 335–357.
- Platt, T., and W. G. Harrison (1985), Biogenic fluxes of carbon and oxygen in the ocean, *Nature*, **318**, 55–58.
- Press, W. H., S. A. Teukolsky, W. T. Vetterling, and B. P. Flannery (1992), *Numerical Recipes in FORTRAN*, second ed., Cambridge Univ. Press, New York.
- Probyn, T. A., B. A. Mitchell-Innes, and S. Searson (1995), Primary productivity and nitrogen uptake in the subsurface chlorophyll maximum on the Eastern Agulhas Bank, *Cont. Shelf Res.*, **15**, 1903–1920.
- Raimbault, P., G. Slawyk, B. Boudjellal, C. Coatanoan, P. Conan, B. Coste, N. Garcia, T. Moutin, and M. Pujol-Pay (1999), Carbon and nitrogen uptake and export in the equatorial Pacific at 150W: Evidence of an efficient regenerated production cycle, *J. Geophys. Res.*, **104**(C2), 3341–3356.
- Rees, A. P., N. J. P. Owens, M. R. Heath, D. H. Plummer, and R. S. Bellerby (1995), Seasonal nitrogen assimilation and carbon fixation in a fjordic sea loch, *J. Plankton Res.*, **17**, 1307–1324.
- Rees, A. P., I. Joint, M. H. Pinkerton, J. Aiken, and D. A. Pilgrim (2001), Carbon, nitrogen and phosphorus budgets within a mesoscale eddy: Comparison of mass balance with in vitro determinations, *Deep Sea Res., Part II*, **48**, 859–872.
- Robins, D. B., R. P. Harris, A. W. Bedo, F. Fernandez, T. W. Fileman, D. S. Harbour, and R. N. Head (1995), The relationship between suspended particulate material, phytoplankton and zooplankton during the retreat of the marginal ice zone in the Bellinghousen Sea, *Deep Sea Res., Part II*, **42**, 1137–1158.
- Sambrotto, R. N. (2001), Nitrogen production in the northern Arabian Sea during the Spring Intermonsoon and Southwest Monsoon seasons, *Deep Sea Res., Part II*, **48**, 1173–1198.
- Sambrotto, R. N., and B. J. Mace (2000), Coupling of biological and physical regimes across the Antarctic Polar Front as reflected by nitrogen production and recycling, *Deep Sea Res., Part II*, **47**, 3339–3367.
- Savidge, G., and L. Gilpin (1999), Seasonal influences on size-fractionated chlorophyll a concentration and primary production in the north-west Indian Ocean, *Deep Sea Res., Part II*, **46**, 701–723.
- Sharp, J. H., M. J. Perry, E. H. Renger, and R. W. Eppley (1980), Phytoplankton rate processes in the oligotrophic waters of the central North Pacific Ocean, *J. Plankton Res.*, **2**, 335–353.
- Small, L. F., M. R. Landry, R. W. Eppley, F. Azam, and A. F. Carlucci (1989), Role of plankton in the carbon and nitrogen budgets of Santa Monica Basin, California, *Mar. Ecol. Prog. Ser.*, **56**, 57–74.
- Smith, D., M. Simon, A. L. Alldredge, and F. Azam (1992), Intense hydrolytic enzyme activity on marine aggregates and implications for rapid particle dissolution, *Nature*, **359**, 139–142.
- Smith, E. M., and W. M. Kemp (2001), Size structure and the production/respiration balance in a coastal phytoplankton community, *Limnol. Oceanogr.*, **46**, 473–485.
- Smith, W. O., Jr. (1995), Primary productivity and new production in the Northeast Water Polyna during summer 1992, *J. Geophys. Res.*, **100**(C3), 4341–4356.
- Smith, W. O., Jr., and D. M. Nelson (1990), Phytoplankton growth and new production in the Weddell Sea marginal ice zone in the austral spring and autumn, *Limnol. Oceanogr.*, **35**, 809–821.
- Smith, W. O., Jr., I. D. Walsh, B. C. Booth, and J. W. Deming (1995), Particulate matter and phytoplankton and bacterial biomass distributions in the Northeast Water (Greenland) Polyna during summer 1992, *J. Geophys. Res.*, **100**(C3), 4357–4370.
- Smith, W. O., Jr., J. Marra, M. R. Hiscock, and R. T. Barber (2000), The seasonal cycle of phytoplankton biomass and primary productivity in the Ross Sea, Antarctica, *Deep Sea Res., Part II*, **47**, 3119–3140.
- Sokal, R. R., and F. J. Rohlf (1995), *Biometry: The Principles and Practice of Statistics in Biological Research*, third ed., W. H. Freeman, New York.
- Steinberg, D. K., C. A. Carlson, N. R. Bates, S. A. Goldthwait, L. P. Madin, and A. F. Michaels (2000), Zooplankton vertical migration and the active transport of dissolved organic and inorganic carbon in the Sargasso Sea, *Deep Sea Res., Part I*, **47**, 137–158.
- Suess, E. (1980), Particulate organic carbon flux in the oceans—Surface productivity and oxygen utilization, *Nature*, **288**, 260–263.
- Sverdrup, H. U. (1953), On conditions for the vernal blooming of phytoplankton, *J. Cont. Int. Explor. Mer.*, **18**, 287–295.
- Sweeney, C., et al. (2000), Nutrient and carbon removal ratios and fluxes in the Ross Sea, Antarctica, *Deep Sea Res., Part II*, **47**, 3395–3421.
- Tarran, G. A., P. H. Burkill, E. S. Edwards, and E. M. S. Woodward (1999), Phytoplankton community structure in the Arabian Sea during and after the SW monsoon, 1994, *Deep Sea Res., Part II*, **46**, 655–676.
- Treguer, P., D. M. Nelson, A. J. Van Bennekom, D. J. DeMaster, A. Leynaert, and B. Queguiner (1995), The silica balance in the world ocean: A reestimate, *Science*, **268**, 375–379.
- Tremblay, J.-E., B. Klein, L. Legendre, R. B. Rivkin, and J.-C. Theriault (1997), Estimation of f-ratios in oceans based on phytoplankton size structure, *Limnol. Oceanogr.*, **42**, 595–601.
- Varela, D. E., and P. J. Harrison (1999), Seasonal variability in nitrogenous nutrition of phytoplankton assemblages in the northeastern subarctic Pacific Ocean, *Deep Sea Res., Part II*, **46**, 2505–2538.

- Veziņa, A. F., C. Savenkoff, S. Roy, B. Klein, R. Rivkin, J. C. Therriault, and L. Legendre (2000), Export of biogenic carbon and structure and dynamics of the pelagic food web in the Gulf of St. Lawrence: Part 2. Inverse analysis, *Deep Sea Res., Part II*, 47, 609–635.
- Waldron, H. N., C. G. Attwood, T. A. Probyn, and M. I. Lucas (1995), Nitrogen dynamics in the Bellinghousen Sea during the Austral spring of 1992, *Deep Sea Res., Part II*, 42, 1253–1276.
- Ward, B., R. J. Olson, and M. J. Perry (1982), Microbial nitrification rates in the primary nitrite maximum off southern California, *Deep Sea Res.*, 29, 247–255.
- Wassman, P. (1990), Relationship between primary and export production in the boreal coastal zone of the North Atlantic, *Limnol. Oceanogr.*, 35, 464–471.
- Watts, L. J., and N. J. P. Owens (1999), Nitrogen assimilation and the f-ratio in the north-western Indian Ocean during an intermonsoon period, *Deep Sea Res., Part II*, 46, 725–743.
- Welschmeyer, N. A., and C. J. Lorenzen (1985), Chlorophyll budgets: Zooplankton grazing and phytoplankton growth in a temperate fjord and the Central Pacific Gyres, *Limnol. Oceanogr.*, 30, 1–21.
- Welschmeyer, N. A., S. Strom, R. Goericke, G. DiTullio, M. Belvin, and W. Petersen (1993), Primary production in the subarctic Pacific Ocean: Project SUPER, *Prog. Oceanogr.*, 32, 101–135.
- Wheeler, P. A. (1993), New production in the subarctic Pacific Ocean: Net changes in nitrate concentrations, rates of nitrate assimilation and accumulation of particulate nitrogen, *Prog. Oceanogr.*, 32, 137–161.
- Wilkerson, F. P., and R. C. Dugdale (1992), Measurements of nitrogen productivity in the equatorial Pacific, *J. Geophys. Res.*, 97(C1), 669–679.
- Wilkerson, F. P., R. C. Dugdale, and R. T. Barber (1987), Effects of El Niño on new, regenerated, and total production in eastern boundary upwelling systems, *J. Geophys. Res.*, 92(C13), 14,347–14,353.
- Wilkerson, F. P., R. C. Dugdale, R. M. Kudela, and F. P. Chavez (2000), Biomass and productivity in Monterey Bay, California: contribution of the large phytoplankton, *Deep Sea Res., Part II*, 47, 1003–1022.
- Yager, P. L., D. W. R. Wallace, K. M. Johnson, W. O. Smith Jr., P. J. Minnett, and J. W. Deming (1995), The Northeast Water Polyna as an atmospheric CO₂ sink: A seasonal rectification hypothesis, *J. Geophys. Res.*, 100(C3), 4389–4398.
-
- R. A. Armstrong, Marine Sciences Research Center, Stony Brook University, Stony Brook, NY 11794, USA.
- J. P. Dunne and A. Gnanadesikan, NOAA Geophysical Fluid Dynamics Laboratory, Forrester Campus B Site, P.O. Box 308, Princeton, NJ 08542-0308, USA. (john.dunne@noaa.gov)
- J. L. Sarmiento, Atmospheric and Oceanic Sciences Program, Princeton University, P.O. Box CN710, Princeton, NJ 08544, USA.